Rational design of SOD mimics

The evaluation of the therapeutic potential of new cationic Mn porphyrins with linear and cyclic substituents

By

Artak Tovmasyan,[1] Sebastian Carballal,[2] Robert Ghazaryan,[3] Lida Melikyan,[3] Tin Weitner,[1] Clarissa G. C. Maia,[4] Julio S. Reboucas,[4] Rafael Radi,[2] Ivan Spasojevic,[5] Ludmil Benov,[6] and Ines Batinic-Haberle[1*]

[1]*Departments of Radiation Oncology, and* [5]*Medicine Duke University Medical Center, Durham, NC 27710, USA;*

[2] *Departamento de Bioquímica and Center for Free Radical and Biomedical Research, Facultad de Medicina, Universidad de la República, Montevideo, Uruguay;*

[3]*Department of Organic Chemistry, Pharmacy Faculty, Yerevan State Medical University, Armenia;*

[4]*Departamento de Quimica, CCEN, Universidade Federal de Paraiba, Joao Pessoa, PB 58051-900, Brazil;*

[6]*Department of Biochemistry, Faculty of Medicine, Kuwait University, Safat, Kuwait*

SUPPORTING MATERIAL

[*]**Corresponding author**

Ines Batinic-Haberle, PhD
Department of Radiation Oncology
Duke University School of Medicine
Durham, NC 27710.
Tel: 919-684-2101
e-mail: ibatinic@duke.edu

Content

Graphical Abstract

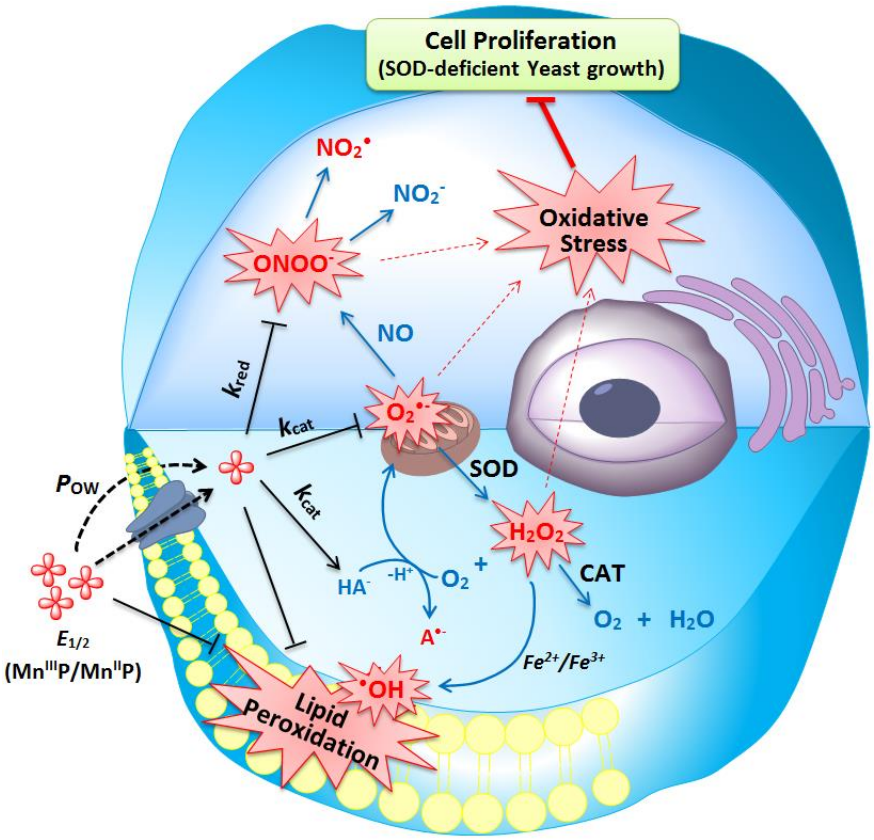

1. Uv-vis spectra of porphyrins and their Mn(III) complexes

The uv/vis spectra were recorded in water at room temperature on a UV-2501PC Shimadzu spectrophotometer with 0.5 nm resolution using a 1 cm quartz cuvette.

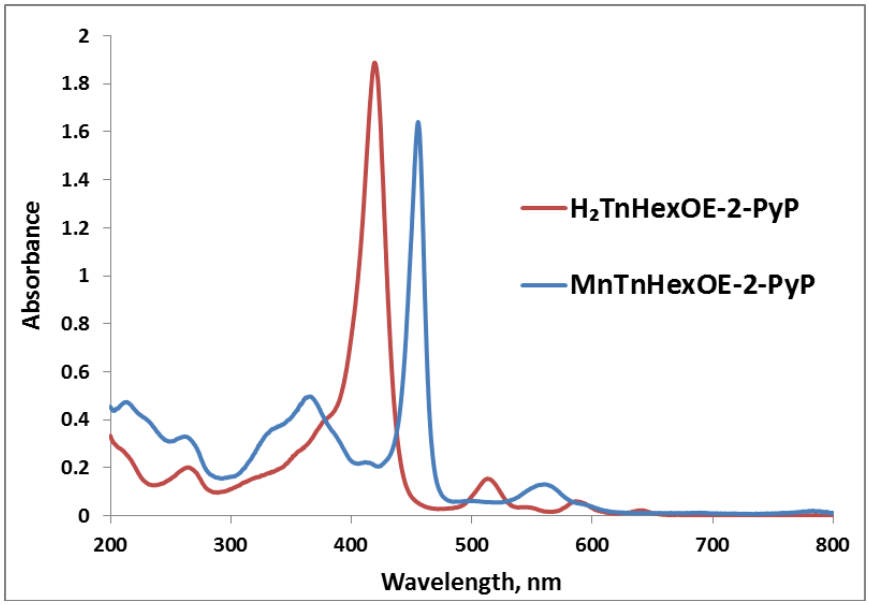

Figure S1. Uv/vis spectra of H_2TnHexOE-2-PyP^{4+} and its Mn(III) complex.

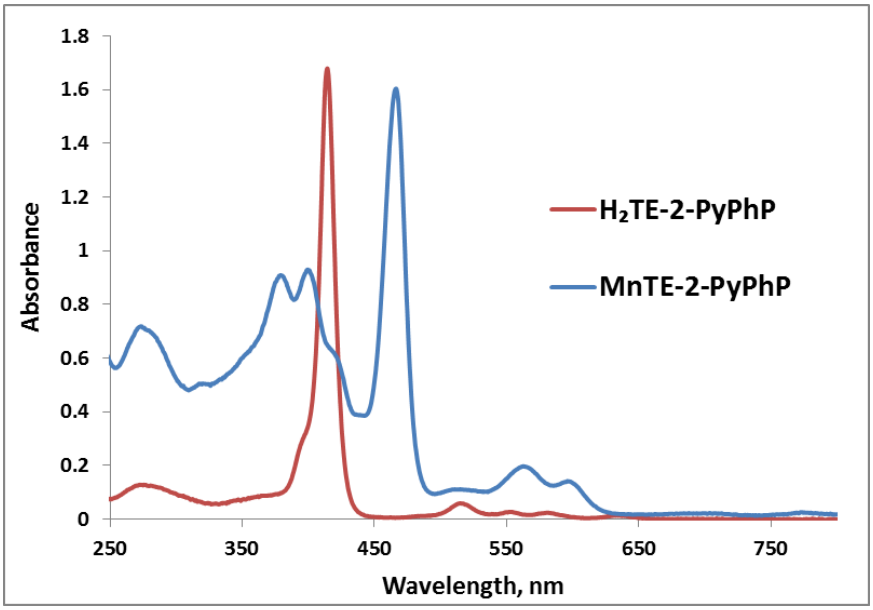

Figure S2. Uv/vis spectra of H_2TE-2-PyPhP^{4+} and its Mn(III) complex.

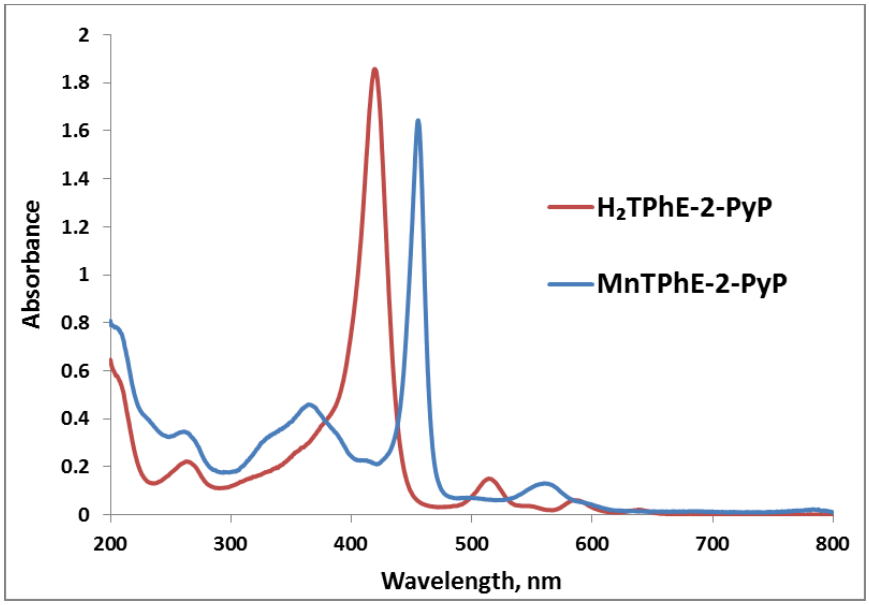

Figure S3. Uv/vis spectra of H_2TPhE-2-PyP^{4+} and its Mn(III) complex.

2. ESI-MS spectra of porphyrins and their Mn(III) complexes

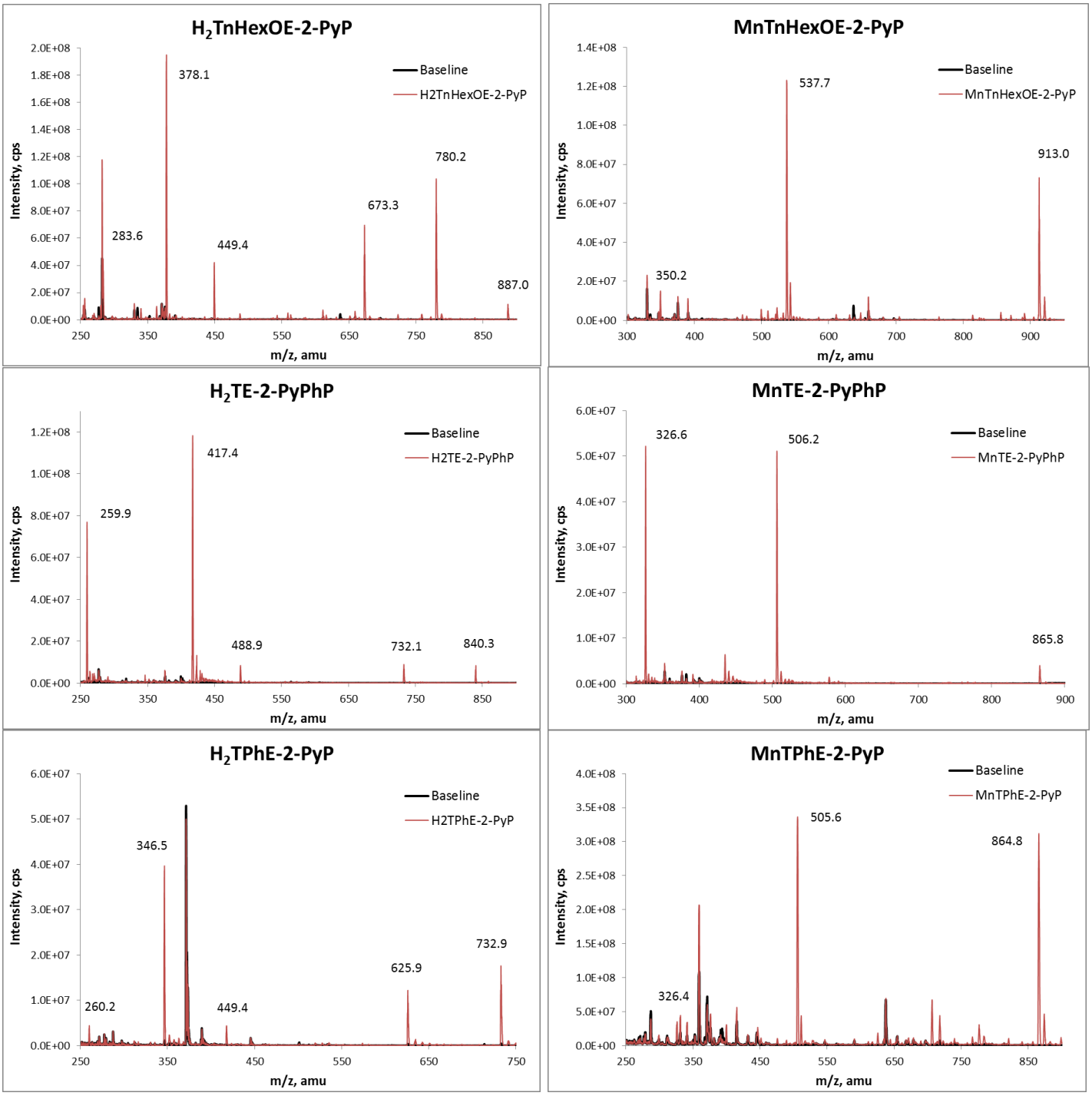

Figure S4. ESI-MS spectra of new porphyrins (H_2TnHexOE-2-PyP^{4+}, H_2TE-2-PyPhP^{4+}, and H_2TPhE-2-PyP^{4+}) and their Mn(III) complexes (MnTnHexOE-2-PyP^{5+}, MnTE-2-PyPhP^{5+}, and MnTPhE-2-PyP^{5+}). ~1 µM sample solution in 1 : 1 v/v acetonitrile : H_2O (containing 0.01% v/v heptafluorobutyric acid (HFBA)) mixture was applied. For peak assignments see **Table 2** in main document.

3. Reduction of peroxynitrite ($ONOO^-$) with Mn(III) complexes

1) MnTE-2-PyPhP^{5+}

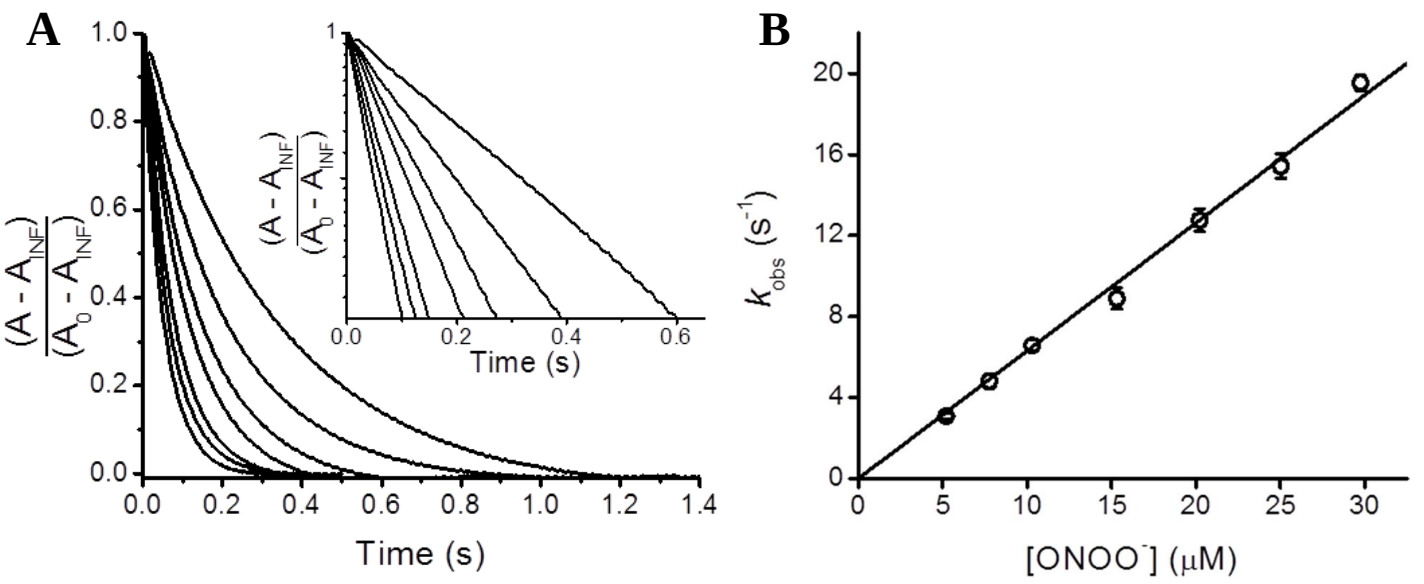

Figure S5. A) Time course of the reaction of MnTE-2-PyPhP^{5+} with peroxynitrite. MnTE-2-PyPhP^{5+} (1 μM) was mixed with peroxynitrite at different concentrations, from right to left: 5.20, 7.76, 10.30, 15.30, 20.21, 25.02 and 29.74 μM, and reaction followed at 467 nm. A is the absorbance at time t, and A_0 and A_{INF} are the initial and final values, respectively. (Inset) Logarithmic plot. **B)** k_{obs} *vs* [$ONOO^-$] plot, which slope is the second-order rate constant for the reaction of peroxynitrite with MnTE-2-PyPhP^{5+}, k_{red}($ONOO^-$). The k_{red} ($ONOO^-$) value is given in the **Table 4** in the manuscript.

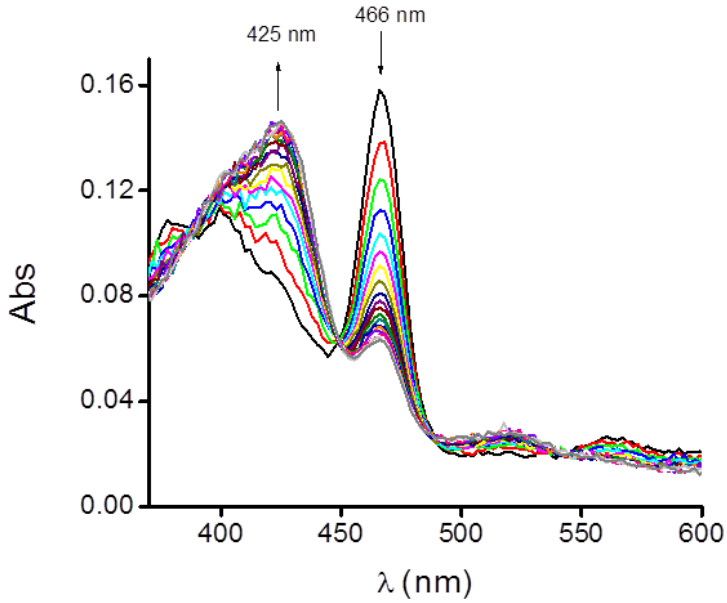

Figure S6. Time-resolved uv/vis absorption spectra obtained upon mixing MnTE-2-PyPhP^{5+} with peroxynitrite. Final concentrations: MnTE-2-PyPhP^{5+} 2 μM, peroxynitrite 20 μM in phosphate buffer (0.05 M, pH 7.3, with 0.1 mM DTPA) at 37 °C. Spectra were collected every 10 ms after mixing, from 0 to 200 ms. The arrows indicate the direction of the absorbance change over time. The isosbestic point indicates the equilibrium between two Mn porphyrin species present in solution: $Mn^{III}P$ and $O{=}Mn^{IV}P$.

2) MnTPhE-2-PyP^{5+}

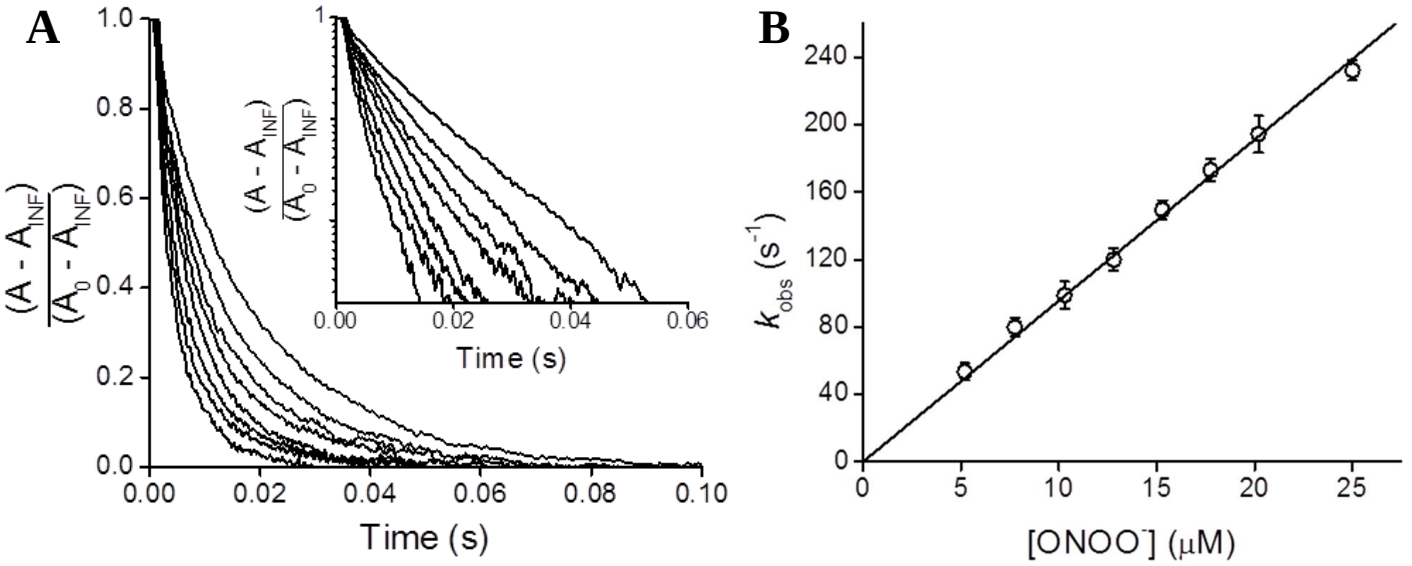

Figure S7. A) Time course of the reaction of MnTPhE-2-PyP^{5+} with peroxynitrite. MnTPhE-2-PyP^{5+} (0.5 μM) was mixed with peroxynitrite at different concentrations, from right to left: 5.20, 7.76, 10.30, 12.81, 15.30, 17.77, 20.21 and 25.02 μM, and followed at 456 nm. A is the absorbance at time t, and A_0 and A_{INF} are the initial and final values, respectively. (Inset) Logarithmic plot. **B)** k_{obs} *vs* [ONOO$^-$] plot, which slope is the second-order rate constant for the reaction of peroxynitrite with MnTPhE-2-PyP^{5+}, k_{red}(ONOO$^-$). The k_{red} (ONOO$^-$) value is given in the **Table 4** in the manuscript.

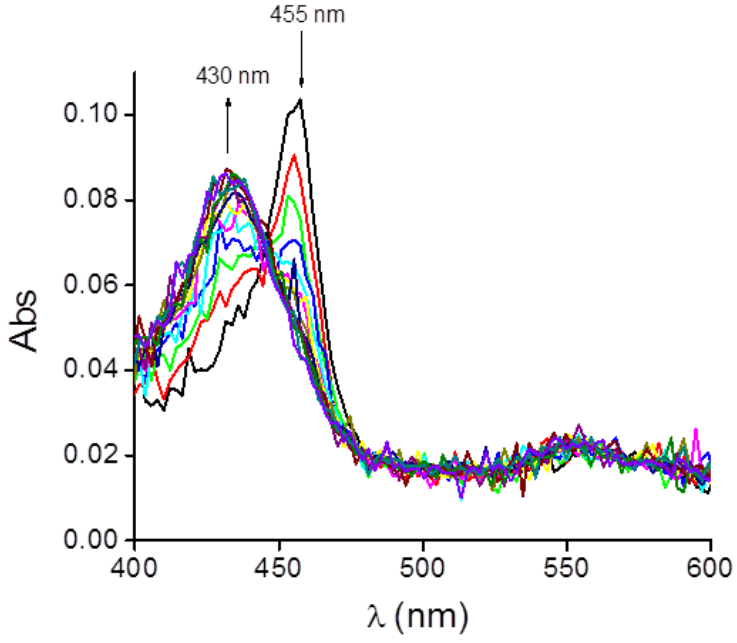

Figure S8. UV-Vis absorption spectra after mixing MnTPhE-2-PyP^{5+} with peroxynitrite. Final concentrations: MnTPhE-2-PyP^{5+} 1 μM, peroxynitrite 10 μM in phosphate buffer (0.05 M, pH 7.3, with 0.1 mM DTPA) at 37 °C. Spectra were collected every 2 ms after mixing, from 0 to 28 ms. The arrows indicate the direction of the absorbance change over time.

3) MnTnHexOE-2-PyP^{5+}

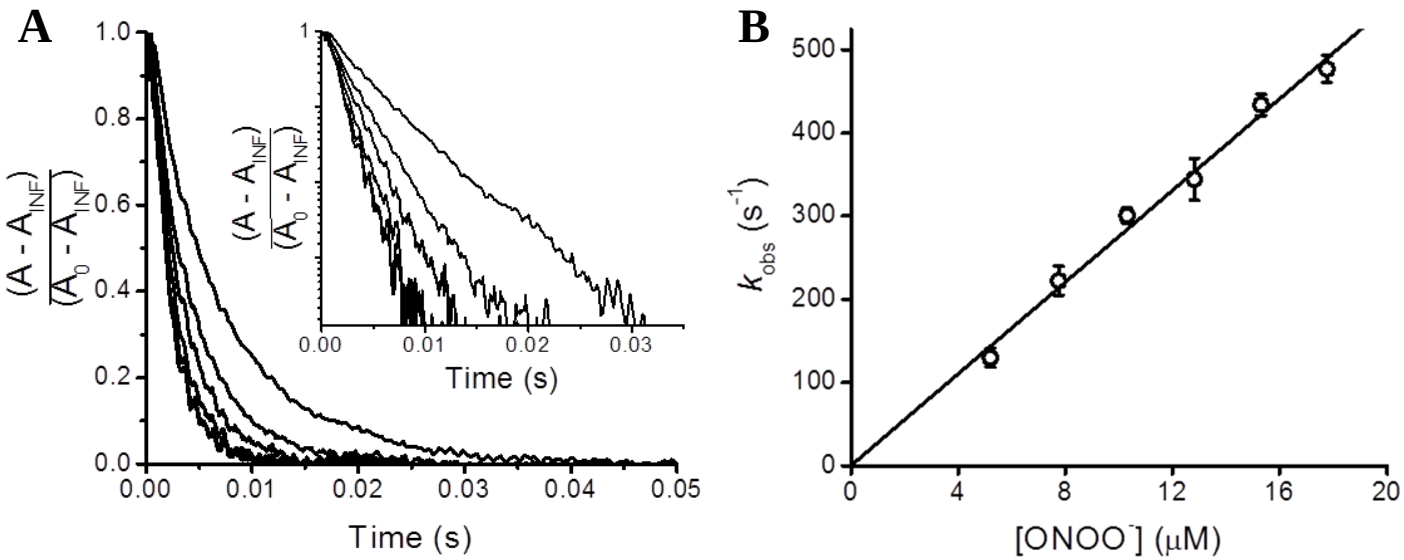

Figure S9. A) Time course of the reaction of MnTnHexOE-2-PyP^{5+} with peroxynitrite. MnTnHexOE-2-PyP^{5+} (0.5 μM) was mixed with peroxynitrite at different concentrations, from right to left: 5.20, 7.76, 10.30, 12.81, 15.30 and 17.77 μM, and followed at 455 nm. A is the absorbance at time t, and A_0 and A_{INF} are the initial and final values, respectively. (Inset) Logarithmic plot. **B)** k_{obs} *vs* [ONOO$^-$] plot, which slope is the second-order rate constant for the reaction of peroxynitrite with MnTnHexOE-2-PyP^{5+}, k_{red}(ONOO$^-$). The k_{red} (ONOO$^-$) value is given in the **Table 4** in the manuscript.

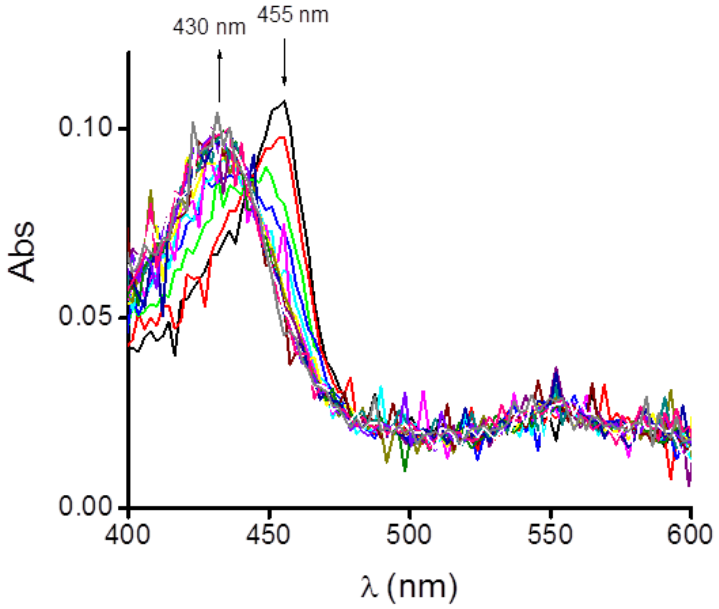

Figure S10. UV-Vis absorption spectra after mixing MnTnHexOE-2-PyP^{5+} with peroxynitrite. Final concentrations: MnTnHexOE-2-PyP^{5+} 1 μM, peroxynitrite 10 μM in phosphate buffer (0.05 M, pH 7.3, with 0.1 mM DTPA) at 37 °C. Spectra were collected every 1 ms after mixing, from 0 to 20 ms. The arrows indicate the direction of the absorbance change over time.

4) MnTE-3-PyP^{5+}

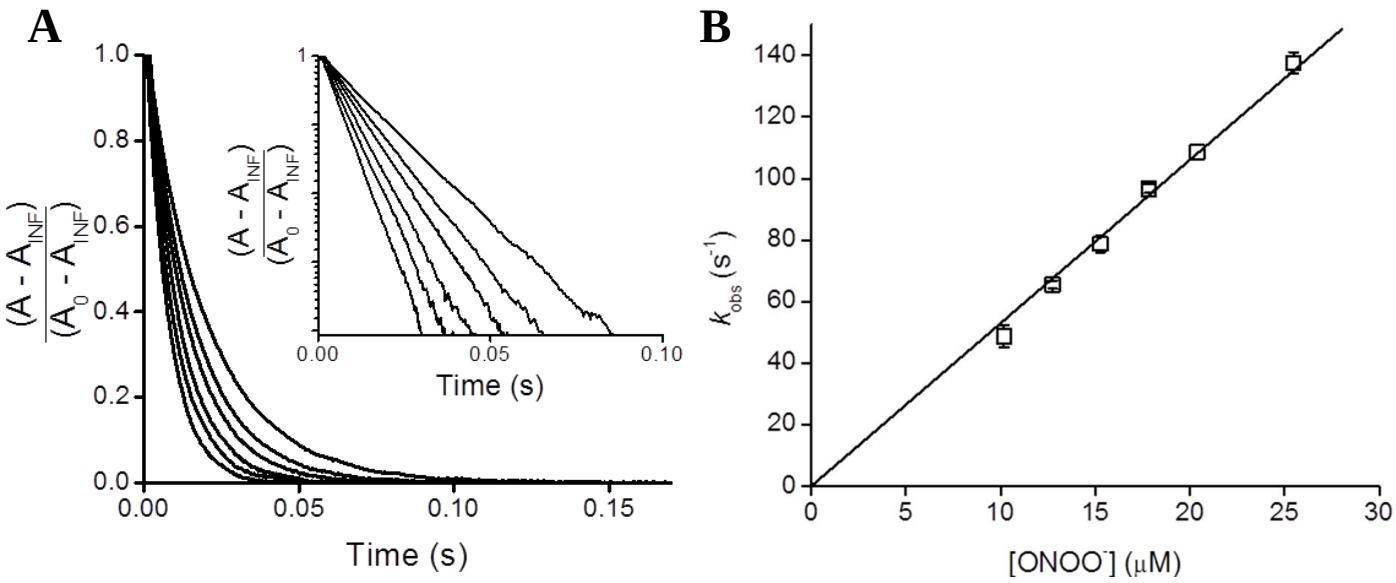

Figure S11. A) Time course of the reaction of MnTE-3-PyP^{5+} with peroxynitrite. MnTE-3-PyP^{5+} (1 μM) was mixed with different peroxynitrite concentrations, from right to left: 10.19, 12.74, 15.28, 17.83, 20.38 and 25.47 μM, and followed at 460 nm. A is the absorbance at time t, and A_0 and A_{INF} are the initial and final values, respectively. (Inset) Logarithmic plot. **B)** k_{obs} *vs* [$ONOO^-$] plot which slope is the second-order rate constant for the reaction of peroxynitrite with MnTE-3-PyP^{5+}. The k_{red} ($ONOO^-$) value is given in the **Table 4** in the manuscript.

4. SOD-like activity of Mn(III) porphyrins

1) MnTE-2-PyPhP^{5+}

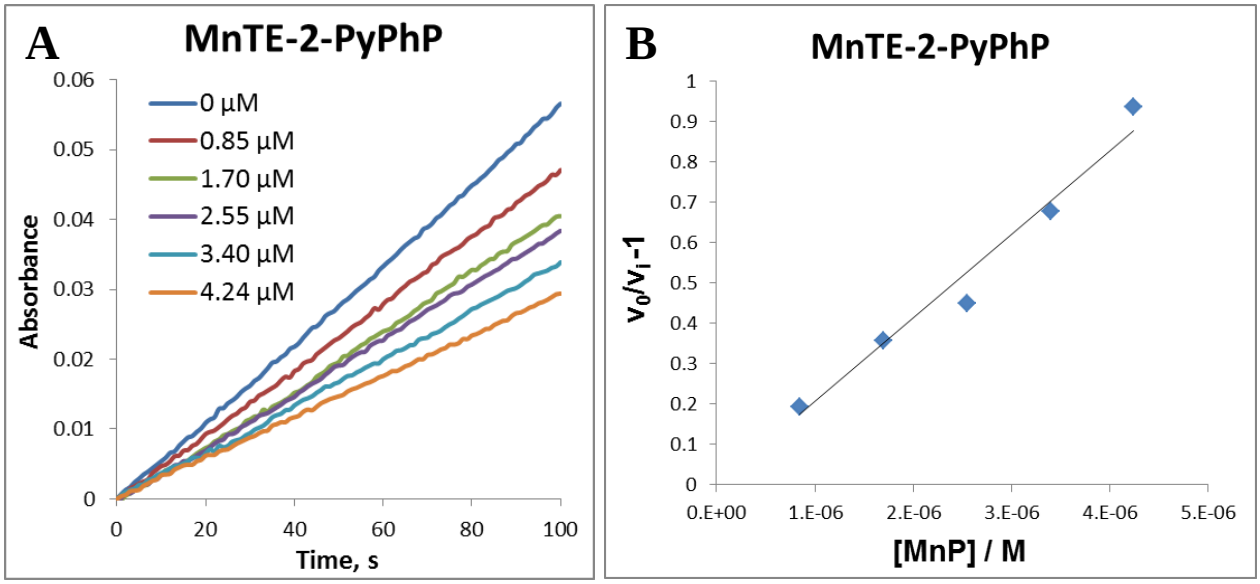

Figure S12. A) Time course of the reaction of MnTE-2-PyPhP^{5+} with $O_2^{\cdot-}$ at (25 ± 1) ^{o}C in 0.05 M potassium phosphate buffer, pH 7.8, 0.1 mM EDTA and at different MnP concentrations. **B)** The plot of (v_0/v_i-1) *vs* [MnTE-2-PyPhP], where v_0 is the rate of reduction of 10 μM cytochrome *c* by $O_2^{\cdot-}$ and v_i is the rate of reduction of cytochrome *c* inhibited by the porphyrin. From the plot, the concentration that causes 50% of the inhibition of cytochrome *c* reduction by $O_2^{\cdot-}$ [IC(50), 1 unit of activity] was found at (v_0/v_i -1) = 1. On the basis of the competition of MnP with 10 μM cytochrome *c*, at 50% inhibition the rates of the reactions of cytochrome *c* and the MnP with $O_2^{\cdot-}$ are equal, i.e., k_{cat} [MnP] = k_{cyt} [cytochrome *c*], where *k*(cyt *c*)= 2.6 × $10^5 M^{-1}$ s^{-1}. This equation allows us to calculate the MnP $k_{cat}(O_2^{\cdot-})$. At any given day of experiments, MnTE-2-PyP^{5+} was always tested along with new compounds to adjust for the fluctuations in methodology (for additional details see [S1].

2) MnTPhE-2-PyP^{5+} and MnTnHexOE-2-PyP^{5+}

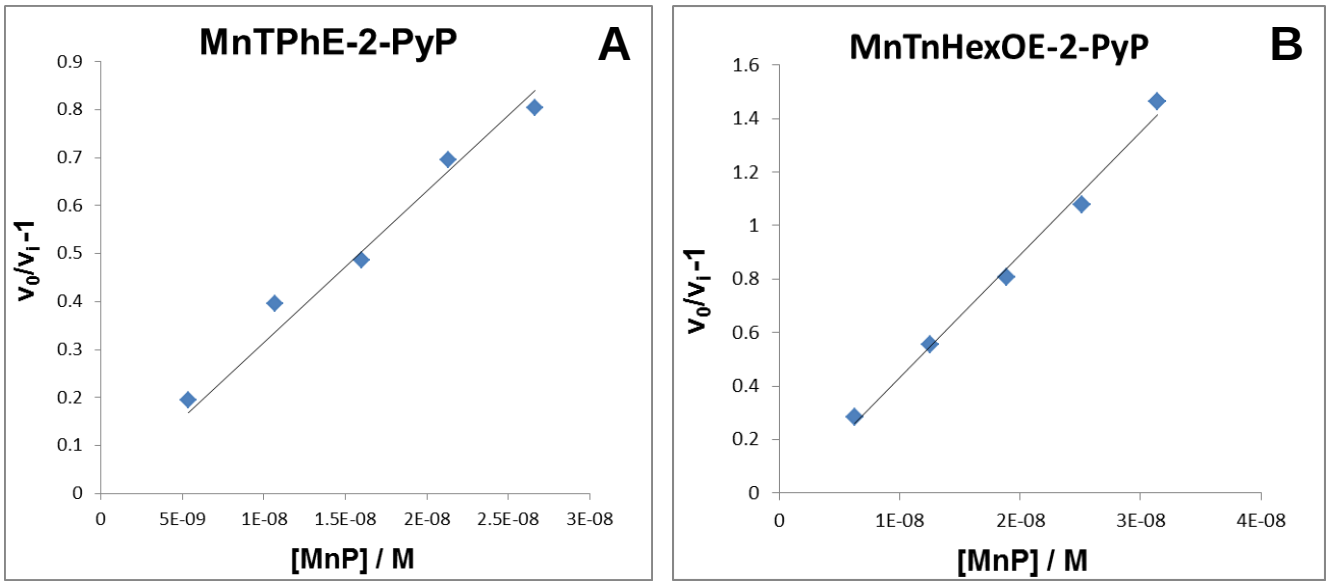

Figure S13. The (v_0/v_i-1) vs [MnP] is plotted for the reactions of MnPs [MnTPhE-2-PyP^{5+} (A) and MnTnHexOE-2-PyP^{5+} (B)] with $O_2^{\cdot-}$ at (25 ± 1) ^{o}C in 0.05 M potassium phosphate buffer, pH 7.8, 0.1 mM EDTA. At any given day of experiments, MnTE-2-PyP^{5+} was tested along with new compounds to adjust for fluctuations in methodology. See in **Figure S12** for the approach to the calculations of $k_{cat}(O_2^{\cdot-})$.

5. The reduction potentials of various couples of Mn(III) porphyrins

Table S1. The reduction potentials of MnPs related to the reduction of Mn from Mn +4 or Mn +5 to Mn +2 or Mn +3 oxidation state in one-electron or two-electron proton-dependent transfers. The data for $O{=}Mn^{IV}P/Mn^{III}P$ and $(O)_2Mn^{V}P/Mn^{III}$ are based on reported values determined at pH 11 [S2-S4]. The $E_{1/2}$ for $Mn^{III}P/Mn^{II}P$ redox couple are from ref [S5,S6].

MnP	$E_{1/2}$ / mV*		
	$Mn^{III}P/Mn^{II}P$ [a]	**$O{=}Mn^{IV}P/Mn^{III}P$ [b]**	**$(O)_2Mn^{V}P/Mn^{III}P$ [c]**
MnTM-2-PyP^{5+}	+220	+540 [d]	~+800 [e]
MnTM-3-PyP^{5+}	+52	+526 [d]	
MnTM-4-PyP^{5+}	+60	+532 [d]	
MnTE-2-PyP^{5+}	+228	+509 [f]	~+800 [e]
MnTE-3-PyP^{5+}	+54	+529 [f]	
MnTnBu-2-PyP^{5+}	+254	+509 [f]	
MnTDM-2-ImP^{5+}	+320		~+800 [e]

* NHE refers to 1N strong acid, whereas SHE refers to the hydrogen ion having unit activity and no ionic interactions. The difference at 25ºC is approximately 5.7 mV [S7]. Specifically, the Nernst equation, nFE = -RTlnK, for the reduction defined as $2H^+$ (1N, activity ≈ 0.8) + $2e^- \rightarrow H_2$ (fugacity ≈ 100kPa) at 25ºC yields $E = E^0 - 29.6 \log[1/(0.8)^2]$ for the potential given in mV, and therefore E(NHE) = E(SHE) - 5.7mV.

[a] Values are in mV *vs* NHE at pH 7.4 (references [S5, S6]).

[b] Values are in mV *vs* SHE at pH 11; there is insignificant difference between the values reported *vs* NHE and SHE.

[c] Values are in mV *vs* NHE at pH 11.

[d] Reference [S2].

[e] Reference [S4].

[f] Reference [S3].

6. References

[S1] Spasojevic, I.; Batinic-Haberle, I.; Stevens, R. D.; Hambright, P.; Thorpe, A. N.; Grodkowski, J.; Neta, P.; Fridovich, I. Manganese(III) biliverdin IX dimethyl ester: a powerful catalytic scavenger of superoxide employing the Mn(III)/Mn(IV) redox couple. Inorg Chem 40:726-739; 2001.
[S2] Ferrer-Sueta, G.; Batinic-Haberle, I.; Spasojevic, I.; Fridovich, I.; Radi, R. Catalytic scavenging of peroxynitrite by isomeric Mn(III) N-methylpyridylporphyrins in the presence of reductants. Chem Res Toxicol 12:442-449; 1999.
[S3] Weitner, T.; Kos, I.; Mandic, Z.; Batinic-Haberle, I.; Birus, M. Acid-base and electrochemical properties of manganese meso(ortho- and meta-N-ethylpyridyl)porphyrins: voltammetric and chronocoulometric study of protolytic and redox equilibria. Dalton Trans 42:14757-14765; 2013.
[S4] Lahaye, D.; Groves, J. T. Modeling the haloperoxidases: reversible oxygen atom transfer between bromide ion and an oxo-Mn(V) porphyrin. J Inorg Biochem 101:1786-1797; 2007.
[S5] Batinic-Haberle, I.; Tovmasyan, A.; Roberts, E. R.; Vujaskovic, Z.; Leong, K. W.; Spasojevic, I. SOD Therapeutics: Latest Insights into Their Structure-Activity Relationships and Impact on the Cellular Redox-Based Signaling Pathways. Antioxid Redox Signal 20:2372-2415; 2014.
[S6] Batinic-Haberle, I.; Reboucas, J. S.; Spasojevic, I. Superoxide dismutase mimics: chemistry, pharmacology, and therapeutic potential. Antioxid Redox Signal 13:877-918; 2010.
[S7] Ramette, R.W. Outmoded terminology: The normal hydrogen electrode. J. Chem. Educ 64:885; 1987.